

Article

# Concepts on Train-to-Ground Wireless Communication System for Hyperloop: Channel, Network Architecture, and Resource Management

Jiachi Zhang <sup>1,2</sup> , Liu Liu <sup>1,\*</sup>, Botao Han <sup>1</sup>, Zheng Li <sup>1</sup>, Tao Zhou <sup>1</sup>, Kai Wang <sup>1</sup>, Dong Wang <sup>2</sup> and Bo Ai <sup>1,3</sup>

<sup>1</sup> School of Electronic and Information Engineering, Beijing Jiaotong University, Beijing 100044, China; jiachi\_zhang@bjtu.edu.cn (J.Z.); bthan@bjtu.edu.cn (B.H.); lizheng@bjtu.edu.cn (Z.L.); taozhou@bjtu.edu.cn (T.Z.); 18120133@bjtu.edu.cn (K.W.); boai@bjtu.edu.cn (B.A.)

<sup>2</sup> School of Rail Transportation, Shandong Jiaotong University, Jinan 250357, China; 215020@sdjtu.edu.cn

<sup>3</sup> State Key Laboratory of Rail Traffic Control and Safety, Beijing Jiaotong University, Beijing 100044, China

\* Correspondence: liuliu@bjtu.edu.cn; Tel.: +86-010-51686315

Received: 8 July 2020; Accepted: 17 August 2020; Published: 20 August 2020



**Abstract:** Hyperloop is envisioned as a novel transportation way with merits of ultra-high velocity and great traveling comforts. In this paper, we present some concepts on the key technologies dedicated to the train-to-ground communication system based on some prevailing fifth-generation communication (5G) technologies from three aspects: wireless channel, network architecture, and resource management. First, we characterize the wireless channel of the distributed antenna system (DAS) using the propagation-graph channel modelling theory. Simulation reveals that a drastic Doppler shift variation appears when crossing the trackside antenna. Hence, the leaky waveguide system is a promising way to provide a stable receiving signal. In this regard, the radio coverage is briefly estimated. Second, a cloud architecture is utilized to integrate several successive trackside leaky waveguides into a logical cell to reduce the handover frequency. Moreover, based on a many-to-many mapping relationship between distributed units (DUs) and centralized units (CUs), a novel access network architecture is proposed to reduce the inevitable handover cost by using the graph theory. Simulation results show that this scheme can yield a low handover cost. Then, with regards to the ultra-reliable and low latency communication (uRLLC) traffic, a physical resource block (PRB) multiplexing scheme considering the latency requirements of each traffic type is exploited. Simulation presents that this scheme can maximize the throughput of non-critical mission communication services while guaranteeing the requirements of uRLLC traffic. Finally, in terms of the non-critical mission communication services, two cache-based resource management strategies are proposed to boost the throughput and reduce the midhaul link burden by pre-fetching and post-uploading schemes. Simulation demonstrates that the cache-based schemes can boost the throughput dramatically.

**Keywords:** hyperloop; train-to-ground communication; wireless channel; network architecture; resource management; multiplexing; cache-based strategies

## 1. Introduction

From the development of China's high-speed railway (HSR), it can be learned that high velocity brings about a number of benefits and merits such as shortening the travel time and helping establish socioeconomically balanced societies [1,2]. However, three inevitable factors primarily restrict the further acceleration, i.e., the mechanical resistance as well as the noise stemmed from the wheels and tracks, and the air resistance derived from air friction. According to reference [3], the actual measurement data demonstrates that the aerodynamic drag accounts for a majority of the resistance

(over 80%) as the train proceeds at a velocity of 400 km/h, leading to a great waste of power energy obviously. Moreover, the generated mechanical noise will rise abruptly along with the acceleration (about seventh-order or eighth-order of speed) and become unbearable for passengers. Given above constraints, the maximum velocity of current HSR cannot exceed 600 km/h.

Hyperloop is a novel designed transportation method, which refers to a maglev train (vacetrain) moving forward at near or supersonic speed (1000–4000 km/h) inside a vacuum metal tube [4]. The closed transportation scenario together with maglev technology can yield a new way of transportation with the merits of low mechanical friction, low air resistance, and low noise mode regardless of all weather conditions, not to mention the great conveniences to customers and quality promotion of rail services due to the ultra-high-velocity. As such, maintaining a dependable and reliable communication link is a pivotal issue to guarantee the safe operation of the Hyperloop and provide real-time multimedia information.

Rekindled by a white paper entitled “Hyperloop Alpha” published by Elon Musk in 2013 [5], the Hyperloop receives extensive attention both from academia and industry. In 2016, an American vacetrain company, i.e., Hyperloop One, published the first study of the Hyperloop system, referring to a 28-min link connecting Helsinki and Stockholm [6]. Then, it first tested a full-scale Hyperloop with power propulsion system, braking system, etc., by using a test line in the northern desert of Las Vegas in 2017 [7]. In 2018, Hyperloop Transportation Technologies (HTT) company declared plans to establish Hyperloop lines in Toulouse, France, and Tongren, Guizhou, China [8]. In 2019, China underlined a series of key tasks for building national strength in transportation in a published official document, among which points out that efforts will also be made to develop the technologies of the low vacuum tube (tunnel) high-speed train [9]. Recently, TÜV SÜD published the first completed certification safety guidelines for Hyperloop applications which define the safety-related requirements relevant to this type of technology in 2020 [10]. The guidelines, which detail over 125 system requirements, are like a milestone on the road to maturity and commercialization of Hyperloop.

As a new-born mode of transportation, the research on train-to-ground communication technology of the Hyperloop almost stays at its infancy stage currently. The primary communication challenge is the fast-fading channel along with the frequent handover effects caused by the ultra-high-speed. However, existing railway-dedicated communication including the widespread commercial used Global System for Mobile Communications-Railway (GSM-R) and Long Term Evolution-Railway (LTE-R) can only support a top speed of 500 km/h [11], which is far below the velocity of the Hyperloop. Currently, some military communication systems such as the common data link (CDL) can support a mobile station (MS) with a speed more than Mach 5 (over 6000 km/h) when providing a data rate of 200 kbps for uplink and 234 Mbps for downlink [12]. However, it is economically expensive and nation-security-endangered to deploy such a military communication system. Moreover, the deployment environment of CDL usually refers to a line-of-sight (LOS) scenario without any reflected radio waves, whereas the closed propagation environment will lead to a severe multipath effect.

To our best knowledge, little research on the communication issue has been conducted, among which our team has performed a series of systematic works. In [13], Qiu summarized the challenges as well as communication quality-of-service (QoS) quantitatively and proposed a leaky waveguide solution for wireless coverage. In [14], we proposed two novel structures to reduce the Doppler effect using the distributed antenna system (DAS) method. In [15], Han performed a series of work on the wireless channel analysis, including Doppler shift, power delay spectrum, and multi-input and multi-output (MIMO) capacity, in the vacuum tube scenarios based on the propagation-graph channel modelling theory. However, [14] lacks a channel modelling-based simulation result, and [15] neglects the large-scale characterization, especially in terms of the path loss. As such, we adopt the two-slope path loss model to depict its attenuation trend in this paper. Moreover, the radio coverage analysis of both DAS and leaky waveguide system (LWS) is performed and the corresponding handover judgment conditions are presented herein.

In terms of the network architecture, literature [16] and [17] proposed a novel baseband unit-to-remote radio unit (BBU-RRU) mapping relationship in the criss-cross railway lines for HSRs and presented an optimal baseband units (BBUs) pool selection algorithm. This scheme dedicated to the Hyperloop leads to a high equipment expenditure. Thereby, we apply this scheme in the 5G network architecture for the Hyperloop. Moreover, the trackside CUs can also provide services for public mobile cellular communication in the vicinity, indicating a full use of resources when no vactrain runs inside this cell.

As for the physical resources management (mainly referring to the physical resource of time and frequency domain), the ultra-reliable and low latency communication (uRLLC) in 5G can satisfy the demands of those latency-sensitive communication services by using the flexible numerology [18]. Therefore, the multiplexing of uRLLC and enhanced mobile broadband (eMBB) traffic attracts extensive attention [19–21]. Different from the conventional multiplexing idea, i.e., puncturing the eMBB physical resource block (PRB) in the next mini-slot of the arriving time, we consider the unique required latency of each uRLLC traffic and propose a flexible multiplexing scheme. In our proposal, each uRLLC traffic is assigned to a PRB position within its maximum tolerable latency. A heuristic algorithm is employed to solve the optimization problem considering maximizing the eMBB throughput and minimizing the uRLLC power.

With regards to the passengers Internet resource management, the cache-based algorithm can yield not only a high throughput but also a low transmission latency [22,23]. Herein, we employ the cache in trackside active antenna unit (AAU) and formulate two resource management schemes by using the predictable vactrain trajectory, which can result in a higher throughput performance than the conventional cache-based scheme. Although the cache-based prefetching idea for the HSRs has been explained in our previous work [24], we formulate another resource management scheme dedicated to the video surveillance data, i.e., post-uploading scheme.

These works provide some insights into the design of the communication system, but also with some limitations, e.g., focusing only on parts of the communication procedure. As such, we aim to propose a wireless communication solution that can provide a reliable connection train-to-ground link from several important communication procedures. Moreover, it should be compatible with existing public mobile cellular communication systems not only to reduce the equipment expenditure but also to use mature and low-cost off-the-shelf technologies based on the previous work.

In this paper, we propose a train-to-ground communication system solution dedicated to the Hyperloop, which mainly involves wireless channel, network architecture, multiplexing scheme of the physical resources, and the on-board passengers' Internet resources management. Our contributions are listed as follows:

- (1) In terms of the wireless access method, the challenges of the DAS method are analyzed from the aspect of Doppler effect. Simulation reveals that a severe Doppler shift appears when crossing the trackside antenna. Thereby, the LWS is a better option since it can yield a stable frequency shift compared to DAS. Then, we discuss the radio coverage based on the DAS and LWS.
- (2) To reduce the handover frequency stemmed from the ultra-high speed, a cloud architecture is used to integrate several successive roadside leaky waveguides into a logical cell. Then, a novel access network architecture dedicated to the Hyperloop is proposed based on a many-to-many mapping relationship between DUs and CUs. The graph theory is adopted to alleviate the inevitable handover cost when crossing different cells and the corresponding simulation result is provided.
- (3) As for the coexisting mission-critical and non-critical services, we propose a PRB multiplexing scheme dedicated to the Hyperloop by considering the tolerable latency margin of each type of traffic. Simulation shows this scheme can satisfy the low-latency demand and achieve a large network throughput in the physical layer.
- (4) To boost the on-board users' quality of experience (QoE) as well as alleviate the midhaul link burden, two cache-based resource management strategies, i.e., the pre-fetching and post-uploading

schemes are investigated to cope with such non-critical mission services. Simulation presents that this cache-based scheme can yield an enhancement in throughput.

The remaining part of this paper proceeds as follows: Section 2 presents the train-to-ground communication challenges and analyzes the communication service types in brief. Then, the possibility of two wireless access methods (the DAS and LWS) are assessed based on some simulation results in Section 3. In Section 4, a novel wireless access network architecture is illustrated in detail. As for the mission-critical traffic, the multiplexing approach is used in the physical layer and presented in Section 5. Moreover, two cache-based resource management strategies mainly served for the non-critical services are illustrated based on our proposed network architecture in Section 6. Finally, the conclusions are summarized in Section 7. Some abbreviations and the corresponding definitions are listed in Table 1 for convenience.

**Table 1.** Abbreviations and definitions.

Term	Definition	Term	Definition
HSR	High-Speed Railway	uRLLC	ultra-Reliable Low Latency Communication
GSM-R	Global System for Mobile Communications-Railway	eMBB	enhanced Mobile Broadband
LTE-R	Long Term Evolution-Railway	5G	The 5th generation
LOS	Line-of-Sight	CBTC	Communication Based Train Control System
CU	Centralized Unit	SIL	Safety Integrity Level
DU	Distributed Unit	WDM	Wavelength Division Multiplexing
AAU	Active Antenna Unit	MIMO	Multi-Input and Multi-Output
DAS	Distributed Antenna System	CIR	Channel Impulse Response
LWS	Leaky Waveguide System	PL	Path Loss
LCX	Leaky Coaxial Cable	C-RAN	Cloud Radio Access Network
QoS	Quality of Service	NFV	Network Functions Virtualization
QoE	Quality of Experience	HARQ	Hybrid Automatic Repeat reQuest
KPI	Key Performance Indicator	MEC	Mobile Edge Computing
BER	Bit Error Rate	PSO	Particle Swarm Optimization
PRB	Physical Resource Block	QAM	Quadrature Amplitude Modulation
BBU	Baseband Unit	RRU	Remote Radio Unit

## 2. Communication Challenges and Service Types

### 2.1. Communication Challenges

The communication demands of the Hyperloop differ from the existing rail transportation dramatically, bringing about some new challenges on the train-to-ground communication system. (1) Special channel characterization. If adopting the public cellular network solution, the Doppler shift varies from the maximum to the minimum value rapidly as the Hyperloop travels across the trackside antenna at an ultra-high-speed, resulting in the drastic variation of the received signal [25]. Not to mention the severe penetration attenuation derived from the steel tube and the metal train body. (2) Except for the severe Doppler effect, another challenge caused by the high velocity is the frequent handover. Furthermore, all passengers insides the vactrain body move simultaneously, which leads to a phenomenon of signaling storm when dealing with a group handover. (3) Various types of communication services with strict demands. Different from rail transportation, the Hyperloop needs more types of mission-critical services with stringent requirements to guarantee the safe operation at such an ultra-high-speed. In addition, the passengers expect to enjoy in-journey communication services of good QoS, which requires a sufficient data rate. As such, the coexistence of both mission-critical and non-critical traffic calls for a novel resource allocation algorithm.

Based on the above analysis, it can be learned that current mobile communication systems such as the GSM-R and LTE-R are incapable of dealing with train-to-ground communication challenges of the Hyperloop. Therefore, we put up with some schemes to investigate on this issue, which will be illustrated in the following sections.

## 2.2. Demands and Requirements of Communication Services

The primary task of the communication system research and design is to identify every service type and quantify the corresponding requirements. As a new mode of transportation, the train-to-ground communication of Hyperloop requires a variety of communication services to assure the safe operation. In [13], we have already presented a summary of accurate communication key performance indicators (KPIs), including data rate, end-to-end transmission latency, and bit error rate (BER), which is presented in Table 2.

**Table 2.** Key KPIs of train-to-ground communication services [13].

Data Type	Data Rate/kbps				Latency Requirement/ms				BER			
	CBTC	HSR	Maglev	Hyperloop	CBTC	HSR	Maglev	Hyperloop	CBTC	HSR	Maglev	Hyperloop
<b>Mission-critical services</b>												
TCS	200/train		1000/train		100	50	5	1	$10^{-6}$	$10^{-6}$	$10^{-6}$	$10^{-6}$
OCS							40	40	$10^{-6}$	$10^{-6}$	$10^{-6}$	$10^{-6}$
OVCS	32/channel				100	100	40	40	$10^{-2}$	$10^{-3}$	$10^{-5}$	$10^{-5}$
TOSM	100	200	200	1000	300	150	300	300	$10^{-3}$	$10^{-6}$	$10^{-3}$	$10^{-3}$
VS	6000	4000	4000	18000	300	150	300	300	$10^{-3}$	$10^{-3}$	$10^{-3}$	$10^{-3}$
PIS	UL:100 DL:8000	UL:100 DL:1000	UL:100 DL:1000	UL:100 DL:8000	300	300	300	300	$10^{-6}$	$10^{-3}$	$10^{-6}$	$10^{-6}$
<b>Passenger multimedia services</b>												
-	0.378–3.78 Gbps				-				-			

Generally, the communication service types of the Hyperloop can be divided into two categories: mission-critical services and passenger communication service data from the aspects of the intended applications. The former one is used to ensure the security of train safe-operation and usually refers to the communication served for operation control system (OCS), traction control system (TCS), operational voice communication system (OVCS), video surveillance (VS), train operation status monitoring (TOSM), and passenger information service (PIS). Different from the HSR, the Hyperloop puts up with more stringent requirements on data rate, end-to-end latency, and BER, which can be regarded as the uRLLC requirements in the 5G communication system [26].

As for the passenger service, it mainly involves the service data such as on-vehicle video conference, online games, chatting, live broadcast, etc., generated by passengers, but having little effect on the safe-operation. We mainly consider the high-speed Internet access service with a large bandwidth requirement. Assume a per-passenger requires a data rate of 0.1–1 Gbps for 5G access, mobile user penetration rate of 90%, 5G terminal penetration rate of 80%, an activation rate of 70%, and a use rate of Internet access service to be 50%. Hyperloop has a total passenger capacity of 15. It follows that the total passenger throughput of the train is  $((0.1, 1) \times 70\% \times 50\%) \times (15 \times 90\% \times 80\%) = 0.378\text{--}3.78$  Gbps, which far exceeds the capability of the existing public mobile cellular system [27]. This type of service can be considered as the eMBB communication in 5G. Based on above analysis, we list some important train-to-ground wireless communication KPIs for communication based train control system (CBTC), HSR, Shanghai maglev, and Hyperloop in Table 2 [28,29]. Since detailed descriptions of each service along with the explanations about the KPI values are given in our previous work [13], we just present a brief overview herein.

The mission-critical communication services account for the safe operation of the Hyperloop. Furthermore, they can be divided into two types from an aspect of the action objection: those related to the safety of the train itself (TCS and OCS data) and public safety ones (including OVCS, TOSM, VS, and PIS). Similar to the HSR, all safety-related communication services of Hyperloop should be categorized as the SIL4, the highest safety level that means a catastrophic impact once it happens [27].

With regards to the passenger multimedia services (PMS), the data rate, latency, and BER requirements are not as stringent as that of the mission-critical services. In addition, the communication demands vary among different passengers even for the PMS. For example, most Internet applications of the business users usually involve web browsing and emailing, which requires a less real-time process and a small throughput. The entertainment users generally involve Internet applications requiring a large bandwidth or real-time process, e.g., online games, video, chatting, etc.

### 3. Wireless Channel Analysis

Hyperloop communication applications have strict requirements for QoS metrics, such as data rate, transmission delay, and BER. Due to these factors as well as a desire to use mature and low-cost technology, we use off-the-shelf technologies and add applications to meet specific services and demands.

Exact and detailed broadband wireless channel characterization is a prerequisite for the deployment and performance analysis of the Hyperloop wireless communication system. Moreover, it provides an effective evaluation of further advanced transmission technologies and resource management.

#### 3.1. Distributed Antenna System

The DAS is an explicit way with the merits of easy to deploy and low cost of equipment. As shown in Figure 1, the Hyperloop is equipped with MIMO antenna array for wireless connection to the ground AAUs. The on-board terminals connect with the inside-train antennas via WiFi technology, these antennas converge all terminals signal and forward them to the outside MIMO antennas via cable or vice versa. This two-hop relay structure avoids a radio wave penetration attenuation of the train body, guaranteeing a relatively stable received amplitude. As such, the wireless channel between ground antennas and train antennas is crucial to the communication system performance.

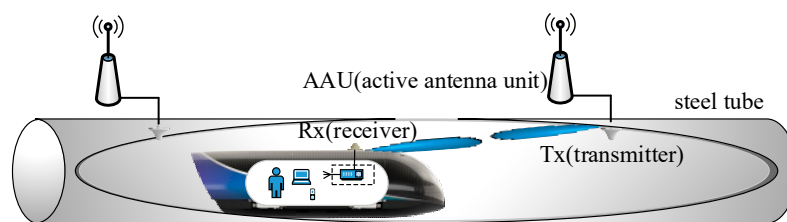


**Figure 1.** The sketch of the distributed antenna system.

In [15], we investigated the wireless channel characterization of this access scheme based on the propagation-graph channel modeling method [30] and obtained some interesting results. In the simulation, the transmitter (Tx) is installed at the inner side of the tube and the receiver (Rx) is set at the top of the train body. To be compatible with existing public mobile cellular communication system, we consider the 5G communication standard and set the bandwidth to 100 MHz and carrier frequency to 4.85 GHz. The shape and size of the tube is set according to [5]. The Hyperloop proceeds at a speed of 1000 km/h traveling across the ground antenna (Tx) located at the middle of the tube.

Figure 2a plots the emulated normalized channel impulse responses (CIRs) at different positions. The strongest received power appears when the Rx arrives at the middle of the tube, i.e., the shortest distance between Tx and Rx. In addition, the number of the effective taps increases as the Hyperloop approaches the ground antenna. The Doppler effect reflects the relative motion between Tx, Rx, and surroundings, which is extremely significant to the channel characterization for the Hyperloop.

Figure 2b shows the Doppler power spectrum considering the LOS, single bounce, and double bounce components. Notably, the shape of the Doppler spectrum presents a feature of central symmetry with the symmetry point lies at the position of ground Tx. The main variation tendency of the LOS component is like as a Z shape with a turning angle close to  $90^\circ$ , whereas the tendency of the multipath component is like a S shape. In addition, their symmetry points vary along with the vactrain's position. In summary, the severe Doppler effect using the DAS can lead to a drastic amplitude variation of the received signal.

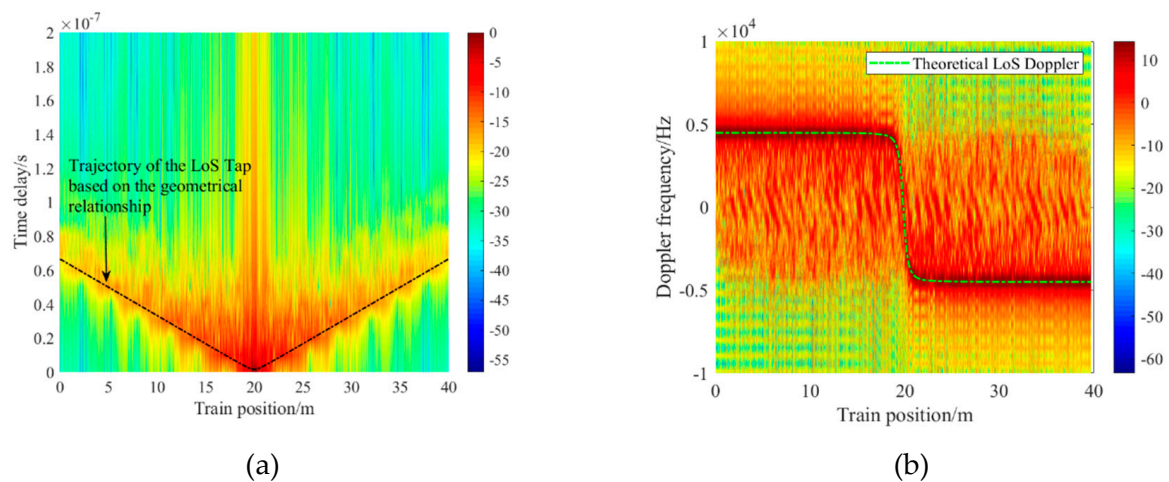


**Figure 2.** Wireless channel analysis results of the DAS: (a) the normalized CIR; (b) the Doppler power spectrums at different positions.

### 3.2. Leaky Waveguide System

Based on the analysis of the DAS results in Section 3.1, the severe Doppler effect will cause a dramatic fast fading effect of the received signals especially in the vicinity of ground antenna. Consequently, it is not suitable to be implemented for the Hyperloop. The LWS and leaky coaxial cable (LCX) are widely used to provide stable and sufficient coverage in the confined space environment [31]. However, LCX cannot support the communication at a high frequency carrier [32]. As such, we utilize the LWS to provide effective radio coverage for the Hyperloop. Figure 3a depicts the access network architecture based on the LWS. The LWS is connected to the road side AAUs via the cable to avoid the penetration attenuation stemmed from the steel tube. A roadside AAU accounts for the signal processing of several leaky waveguides. It is worth noting that the conventional leaky waveguide emits a signal of which the equiphase surface direction is not perpendicular to train movement direction as shown in Figure 3b. This phenomenon is caused by the fact that the currently used leaky rectangular waveguide uses fast waves as the fundamental mode to generate radiation. The Doppler frequency shift of the LOS component can be expressed as  $f_d = v_0 \cos \theta / \lambda$ , where  $v_0$  is the velocity and  $\lambda$  is the wavelength. Obviously, the  $f_d$  keeps a constant as long as  $v_0$  does not change. Then, some off-the-shelf frequency compensation algorithms can be used to handle this situation directly. Note that the AAU connect to all leaky waveguides at the same side (left/right), otherwise, the Doppler shift will change from  $f_d$  to  $-f_d$ .

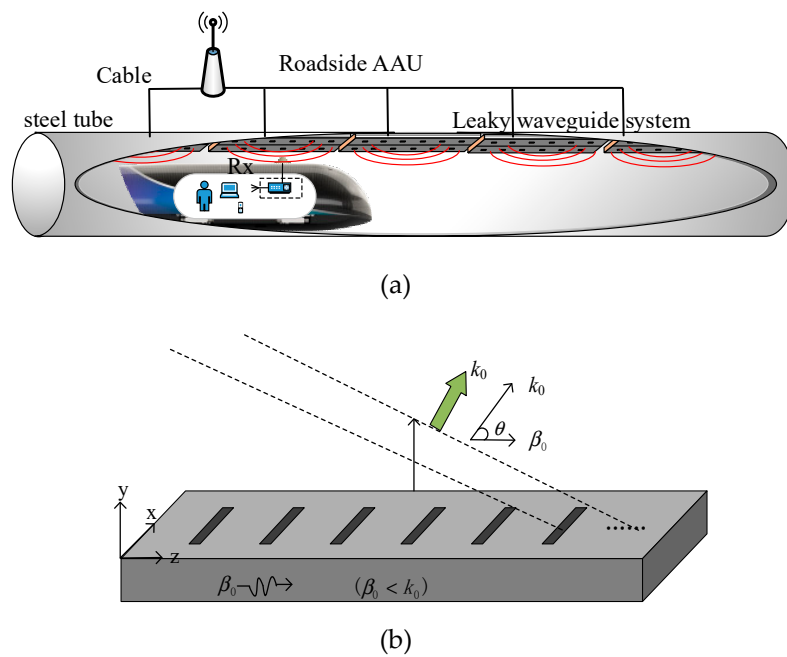


**Figure 3.** The leaky waveguide system: (a) a schema; (b) the radio propagation direction.

### 3.3. Radio Coverage Analysis

To cope with the handover when employing either the DAS or the LWS, it is essential to analyze the effective radio coverage. As for the LWS, the radiated power stemmed from a slot can be expressed as

$$P = P_0 e^{-\beta z}, \tag{1}$$

where  $P_0$  is the transmit power,  $z$  means the distance from starting position of the leaky waveguide to the slot position.  $\beta$  is an attenuation constant with a low value [33]. In terms of the DAS, numerous references (e.g., [34]) state that the received power curve is divided into two regions, typically referred to as near and far region, i.e., the two-slope channel model. Two-slope channel models are typical representative of numerous empirical models based on measurements of the received signal strength, which is expressed as

$$P = \begin{cases} P_0 e^{-\beta z}, & 0 \leq z \leq D \\ P_0 e^{-\alpha_N D} \cdot e^{-\alpha_F(z-D)}, & z > D \end{cases} \tag{2}$$

In the near region, the PL slope  $\alpha_N$  is steep, which is usually modeled as free space path loss. In the far region, the waveguide effect appears with few lower order modes and the path loss slope is reduced significantly, denoted as  $\alpha_F$ . The break point, which is a point of transition from near to far region, can be estimated by  $D = a^2/\lambda$ , where  $a$  is the maximum transverse dimension of the tube and  $\lambda$  is the signal wavelength in free space [34].

Based on Equations (1) and (2), Figure 4 plots the demonstration of the handover process of both LWS and DAS between two adjacent cells.  $D_{eff-L}$  and  $D_{eff-D}$  mean the effective coverage of the LWS and DAS, respectively. The handover will occur once it satisfies the A3 judgment condition, which is usually adopted in LTE-R [35].

$$M_n + Of_n + Oc_n - Hys > M_s + Of_s + Oc_s + Off, \tag{3}$$

where  $M_s/M_n$  is the signal quality of source/target AAU,  $Of_s/Of_n$  is the specific frequency offset of source/target AAU,  $Oc_s/Oc_n$  is the specific offset of source/target AAU.  $Off$  is the offset parameter,

and  $Hys$  is the hysteresis parameter. Obviously,  $M_s$  and  $M_n$  are determined by the PL. Given that  $\beta < \alpha_F < \alpha_N$  and  $D = a^2/\lambda$ , the  $D_{eff-L}$  and  $D_{eff-D}$  can be expressed as based on Equation (3),

$$P_0 e^{-\beta(z-z_{L0})} + Of_n + Oc_n - Hys > P_0 e^{-\beta(z_{L1}-z)} + Of_s + Oc_s + Off, \quad (4)$$

$$P_0 e^{-\beta(z-z_{L0})} + Of_n + Oc_n - Hys > P_0 e^{-\beta(z_{L1}-z)} + Of_s + Oc_s + Off. \quad (5)$$

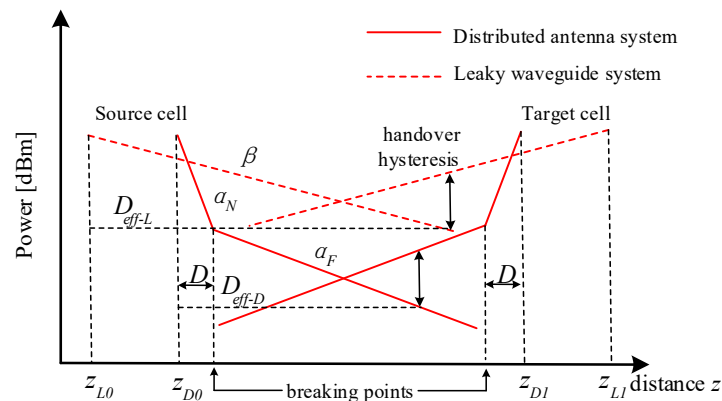


**Figure 4.** The handover process based on the DAS and LWS.

Based on Equations (4) and (5), the radio coverage of the DAS and LWS between two adjacent cells when processing the handover can be calculated. Obviously,  $D_{eff-L}$  is usually larger than  $D_{eff-D}$  since the received power slope of the DAS is sharper than that of the LWS. Considering that the effective radio coverage of a single AAUs is a constant, one trackside AAU connects to more antennas than that of the leaky waveguides consequently. In addition, the handover failure probability of DAS is higher than that of the LWS. On one side, it can be explained by the low received signal strength of the DAS, on the other hand, this phenomenon derives from the drastic signal variation caused by the time-varying Doppler shift. In conclusion, the LWS is a better wireless access method option compared to the DAS, except for the high expenditure cost.

#### 4. Network Architecture

The other primary challenging issue stemmed from the ultra-high-speed is the extremely frequent handover, which is an integral part of every mobile communication system. For instance, the maximum cell range in LTE-R is 12 km, the residence time inside a cell is about 43.2 s at a velocity of 1000 km/h. Currently, numerous in-depth research has been conducted to alleviate the performance degradation caused by the handover from a variety of aspects such as computing power or handover protocols. For example, in [36], Zhao proposed a dual-link soft handover scheme for C/U plane split network in HSR by deploying a train relay station and two antennas on the train. In [37], Song proposed a handover trigger decision scheme by using the grey system theory to predict the received signal quality. These works can cope with the handover issue efficiently; however, it needs the assistance of multi-links to achieve a high-reliable handover. Hence, it is hard to implement these schemes for the Hyperloop since the leaky waveguide system emits a signal that can hardly affect the nearby cells.

Network architecture refers to the way network devices and services are structured to serve the connectivity needs of client devices. A good network architecture can provide sufficient communication QoS at a low equipment cost and supports flexible configuration for diverse demands. Moreover, it can reduce the inevitable handover cost if possible. However, it is economically expensive to establish a new dedicated access network for the Hyperloop. Therefore, we aim to establish a network architecture based on the 5G architecture not only to provide the communication services for the Hyperloop, but also can be compatible with roadside public cellular networks.

#### 4.1. Centralized Access Architecture

Cloud radio access network (C-RAN) is considered as a promising solution to provide high communication services in the high-speed mobile scenario as it is a clean, centralized processing, collaborative radio, and real-time cloud computing infrastructure wireless access architecture [38]. As such, we utilize the C-RAN architecture for the Hyperloop communication based on the 5G network.

Generally, the C-RAN in 5G system consists of three functional entities, i.e., trackside ground AAUs, centralized units (CUs), and distributed units (DUs) [39]. The CU mainly processes the non-real-time wireless high-level protocol, i.e., radio resource management and dual connection. CUs can be deployed on a general hardware platform together with mobile edge computing. A DU mainly processes physical layer functions and the real-time hybrid automatic repeat request (HARQ) flow through a dedicated equipment platform or a general + dedicated hybrid platform. The AAU contains parts of physical layer function and all radio frequency (RF) functionality, such as the transmit and receive functions, filtering, and amplification. With the merits of easy-to-install, the compact AAUs are distributed along the line evenly to realize seamless wireless coverage. Considering the stringent uRLLC services demands, the roadside AAUs and DUs are integrated into one entity. The CUs together with mobile edge computing (MEC) platform and parts of the core network functions are located near the Hyperloop lines, which is called the edge cloud. Network functions virtualization (NFV) technology is used for the edge cloud by decoupling the network functions from proprietary hardware appliances [40]. Hence, the edge cloud runs in software on standardized computer servers. Usually, a handover involves the participation of the core network. By migrating parts of core network function to the edge cloud, it can reduce the latency evidently, which caters to the demands of uRLLC traffic. The AAUs connect with the DUs via the midhaul, whereas the DUs are connected to the CUs via the F1 interface, i.e., the midhaul.

Figure 5 presents a diagram of the C-RAN for the Hyperloop. The nearby AAUs connect with the LWS via the cable and forward data to the edge cloud (or vice versa). The on-board terminals connect with the antennas embedded inside the train via WiFi technology, these antennas converge all terminals signal and forward them to the outside multi-input and multi-output (MIMO) antennas via cable or vice versa. This two-hop relay structure avoids a radio wave penetration attenuation of the vactrain body, guaranteeing a relatively stable received amplitude. The edge cloud can obtain a timely and accurate information of the train position based on the monitoring and detecting devices distributed along the tube line. As such, it can enable the approaching cell and disable the passing one as the train proceeds forward. This is the basic idea of the moving cell scheme, which integrates several adjacent AAUs connecting to the same edge cloud into a logical cell to achieve a free-handover effect [41].

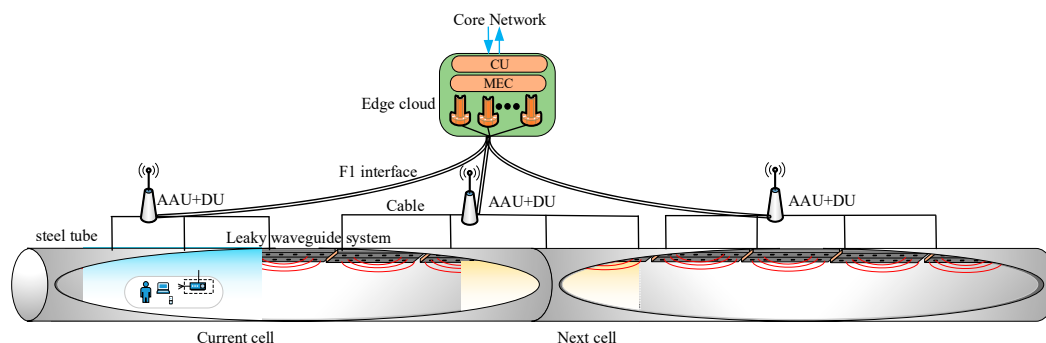


**Figure 5.** The diagram of the C-RAN architecture for Hyperloop.

Despite the fact that this architecture can cope with the frequent handover efficiently, this benefit will disappear as the Hyperloop travels across two edge clouds. This challenging issue will be addressed in the following section.

#### 4.2. A Novel Network Architecture

To handle the inevitable handover during a long Hyperloop line, some improvements are proposed to boost the communication performance therein. As traveling across two adjacent edge clouds during a long-distance Hyperloop line, the inevitable cloud-to-cloud handover yields a certain resource migration cost. Hence, we aim to reduce the cost as much as possible by extending the CU–DU mapping relationship to a more flexible one. Generally, one edge cloud connects to several roadside AAUs + DUs through the F1 interface [39], whereas a single AAU + DU can only connect to one edge cloud, i.e., one-to-many mapping relationship [16]. Given the fact that it is economically expensive to establish a dedicated network to the Hyperloop, the communication system deployed along the Hyperloop line should also provide communication services to the nearby public cellular system or the nearby other railway lines to make full use of the equipment resources. In this regard, we upgrade the star architecture to a flexible mesh architecture. In other words, one AAU + DU can connect to more than one edge cloud in its neighbor, i.e., the many-to-many mapping relationship.

Figure 6 shows the diagram of the proposed network architecture, where Figure 6a is a schema of the conventional one-to-many mapping relationship and Figure 6b presents the many-to-many mapping relationship. Compared to Figure 6a, the many-to-many architecture enables a more flexible handover scheme. In addition, this flexible meshed architecture can yield a high safety robustness. For instance, if the link connecting cloud 1 to 3 suffers an interruption accidentally, the Hyperloop can still maintain an uninterrupted connection via the link from cloud 1 to 2 and link from cloud 2 to 3.

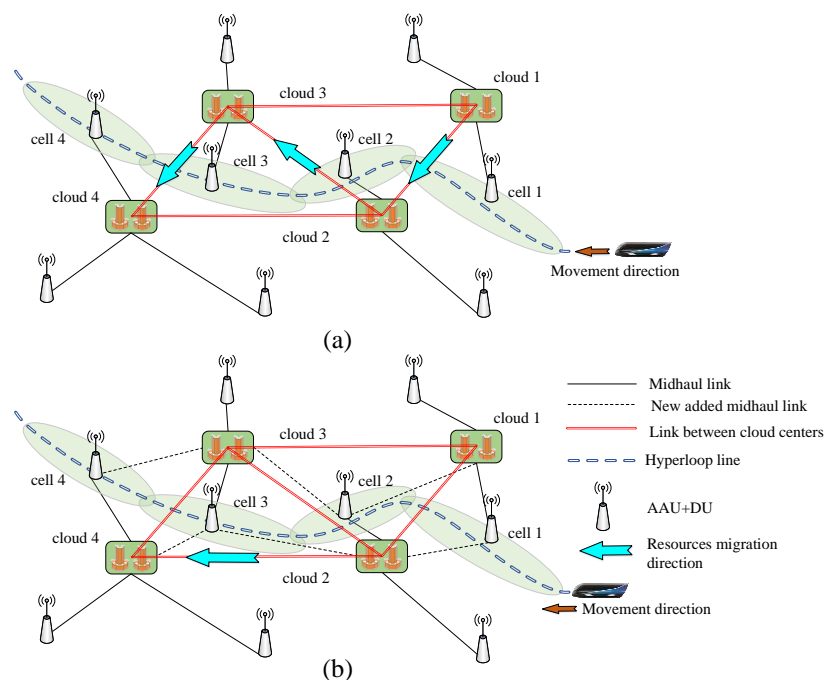


**Figure 6.** The diagram of the network architecture: (a) one-to-many; (b) many-to-many.

As the Hyperloop proceeds inside a cell, it will choose an edge cloud to communicate according to each cloud's real-time computational burden status as well as the topography structure. The burden status of the cloud center varies at different time even without the Hyperloop. However, compared to the ultra-high-speed of the Hyperloop, the burden status can be regarded as static within a short interval. During this interval, assume the Hyperloop travels across several cells involving  $N_T$  edge clouds. Consider the cloud-to-cloud handover, a weighted undirected graph can be established by abstracting the cells and edge clouds into vertex sets and abstracting the cloud-to-cloud links into edge sets.

As shown in Figure 6, the Hyperloop proceeds across from cell 1 to 4 successively, involving 4 nearby edge clouds, i.e., cloud 1 to 4. Figure 7 presents an abstract graph of this topographical relationship. The vertical direction means the successive passing cells along the Hyperloop line, whereas the horizontal direction denotes cloud centers. Those vertexes with deep color in one row refer to those edge clouds that are connected to the same cell. The numbers marked inside each vertex circle denote the currently available computational capability of the edge cloud. As the Hyperloop travels across two cells belonging to two different edge clouds, a group handover occurs with a resource migration cost (e.g., the drop rate, BER, throughput, etc.). The cost  $g_{cc'}$  between edge cloud  $c$  and  $c'$  can be calculated as

$$g_{cc'} = \begin{cases} 0, & c = c' \\ N_a D'_{cc'} / F'_{cc'}, & c \rightarrow c' \\ +\infty, & c \rightarrow c' \end{cases} \quad (6)$$

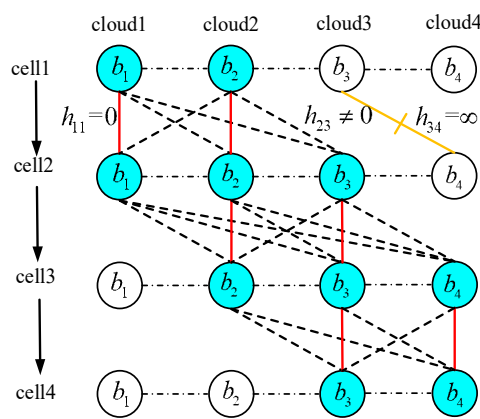


Figure 7. The schematic diagram of graph theory.

In Equation (6), the first case indicates that no handover occurs within the same edge cloud, i.e.,  $c = c'$ . The second case means that the cost is proportional to the active passenger number  $N_a$  as well as the normalized distance  $D'_{cc'}$  between these two clouds and inversely proportional to the normalized capacity of the clouds' link  $F'_{cc'}$ . The third case infers that two clouds that are not physically linked cannot perform a handover.

Another consideration when selecting the cloud is the corresponding available computational capacity since a heavy-burdened edge center may reduce the processing efficiency of the Hyperloop communication tasks. As such, the total handover cost should be a sum of these two costs, which can be marked as  $\eta g_{cc'} + (g_c + g_{c'})$ , where  $\eta \in (0, 1)$  is a constant used to tune the primary of these two costs.

Finally, our goal is to minimize the total group handover cost during the whole Hyperloop line by selecting a certain edge center at different logical cells, which can be expressed as

$$\min_{\varphi_{l,c}, \varphi_{(l+1),c'}} \left\{ \sum_l \eta \varphi_{l,c} \varphi_{(l+1),c'} g_{cc'} + (\varphi_{l,c} g_c + \varphi_{(l+1),c'} g_{c'}) \right\} \quad (7)$$

where  $\varphi_{l,c} \in \{0, 1\}$  denotes the selection variable that the logical cell  $l$  selects the cloud  $c$  to communicate as the Hyperloop travels inside it and  $\varphi_{(l+1),c'}$  represents the selection of the next logical cell  $(l + 1)$ . The selection variables are constraint by following formulas

$$\sum_c \varphi_{l,c} = 1, \quad (8)$$

$$\sum_{c'} \varphi_{(l+1),c'} = 1, \quad (9)$$

which means that one logical cell can only select one edge cloud to communicate as the Hyperloop travels inside it. Optimization problem (7) together with Equations (8) and (9) can be regarded as an NP-hard problem and it can be solved by the Floyd–Warshall algorithm. Details solution can be found in our previous work [16,17]. Based on the proposal, the group handover cost can be alleviated evidently to ensure a high on-board communication QoS together with reliable and safe operation of the Hyperloop.

## 5. Wireless Physical Resources Management

Based on the aforementioned analysis in Section 2, the two main types of communication services, i.e., the mission-critical service and passenger Internet service can be categorized as the eMBB and uRLLC services. Since these two application cases are supported simultaneously in 5G, the joint physical resource scheduling of eMBB and uRLLC traffic is another challenging issue to the Hyperloop. Thanks to the flexible frame structure of the 5G, a time slot can be divided into several mini-time slots to cope with the uRLLC traffic. The concept of multiplexing is to deal with these two coexisting services by puncturing/superposing parts of PRBs assigned to eMBB traffic for the sporadically arrived uRLLC packets at the next mini-slot boundaries [19].

Currently, much work about multiplexing has been investigated, such as [19–21], which mainly aim to boost the throughput of the eMBB services subject to the instant puncturing of the uRLLC traffic on the eMBB packet transmission upon arrival. However, the primary issue of these research is that all sporadically arrived uRLLC traffic are treated equally without any discrimination. Consequently, these methods cannot process the multiple types of uRLLC traffic with different KPIs for Hyperloop and that is the issue we try to solve.

Figure 8 presents a diagram of the proposed wireless PRB multiplexing of the eMBB and uRLLC traffic. As shown in this figure, each time slot with one millisecond time duration is divided into  $M$  mini-slots equally so as to achieve the stringent latency requirement of uRLLC. Four different colors represent 4 eMBB services users, which are scheduled at the slot boundary periodically. In addition, the proportional fairness algorithm is adopted to guarantee the data rate fairness among different users. Three types of the uRLLC traffic arrive sporadically during the time slot whose PRBs are already allocated to different eMBB users and should be processed before the next time slot due to the strict latency requirements.

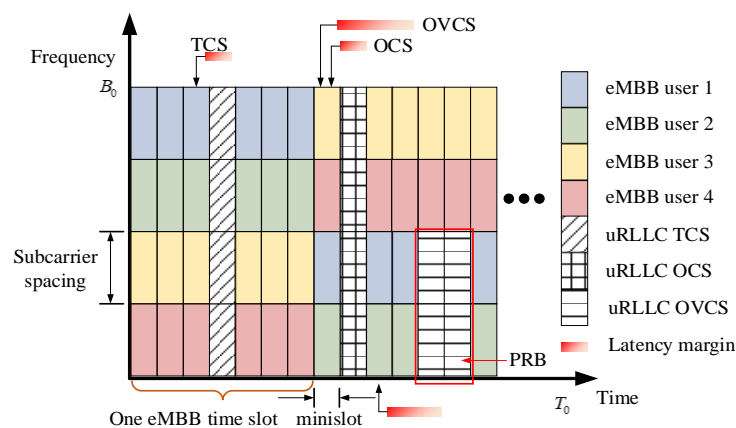


**Figure 8.** The diagram of the physical resource multiplexing of the eMBB and uRLLC.

Given the fact that the 5G supports a flexible frame structure, each type of uRLLC traffic can be allocated to a PRB with specific bandwidth and time duration [18]. Specifically, a traffic with a stringent latency requirement is allocated to a PRB with small time duration but large bandwidth. To cope with the multi-types of uRLLC traffic for Hyperloop, we propose a novel latency-margin-based multiplexing scheme herein. In contrast to the conventional multiplexing scheme, multi-types of uRLLC traffic will be processed not at the next mini-slot directly. Instead, it is permitted to be allocated

within its corresponding latency margin. For instance, two different types of uRLLC traffic arrive at the eighth mini-slot in Figure 8, the system ought to deal with OVCS traffic in no longer than next three mini-slots (latency margin: three mini-slots), whereas it would cope with the TCS and OCS traffic within next mini-slot (latency margin: one mini-slot). Obviously, the latency-margin-based idea enables great puncturing flexibility of PRB when multiplexing.

The goal of the proposed latency-margin-based multiplexing scheme is to maximize the throughput of all eMBB traffic and minimize the allocated power of the uRLLC traffic when guaranteeing the latency and BER demands of the sporadically arrived uRLLC traffic. Let  $n_0$  denote the channel noise power,  $h_{t,f}$  means the channel gain of the PRB at the  $t$ -th mini-slot and  $f$ -th subcarrier. Several  $M$ -quadrature amplitude modulation (QAM) modes can be chosen based on the BER and data rate requirements as well as the channel gain  $h_{t,f}$ . Then, this optimization problem can be expressed as

$$\min_{t_q, f_q, p_{t_q+i, f_q+j}^s} \{\alpha T^{\text{uRLLC}} + \beta P^{\text{uRLLC}}\}, \quad (10)$$

$$\text{s.t. } T^{\text{uRLLC}} = \sum_{q=1}^Q \sum_{i=1}^{N_q^t} \sum_j^{N_q^f} \Delta f \Delta t \log_2 \left( 1 + \frac{p_{t_q+i, f_q+j} h_{t_q+i, f_q+j}}{n_0 \Delta f} \right) \quad (11)$$

$$P^{\text{uRLLC}} = \sum_{q=1}^Q \sum_{j=0}^{N_q^f} \sum_{i=0}^{N_q^t} p_{t_q+i, f_q+j} \quad (12)$$

$$P_q^s(M, \gamma_q) \leq P_q^{\text{require}} \quad (13)$$

$$p_{t_q+i, f_q+j} = \frac{p_q \|h_{t_q+i, f_q+j}\|^2}{\sum_{j=0}^{N_q^f} \sum_{i=0}^{N_q^t} \|h_{t_q+i, f_q+j}\|^2} \quad (14)$$

$$\gamma_q = \frac{\sum_{j=0}^{N_q^f} \sum_{i=0}^{N_q^t} p_{t_q+i, f_q+j} |h_{t_q+i, f_q+j}|^2}{N_q^t N_q^f \Delta f} \quad (15)$$

$$(t_{q+i}, f_{q+j}) \cap (t_{q'+i'}, f_{q'+j'}) = \emptyset; q \neq q'; q, q' \in \{1, 2, \dots, Q\} \quad (16)$$

$$0 \leq t_q - t_{arr} \leq d_q, t_q \in \mathbb{N}^* \quad (17)$$

$$1 \leq f_q \leq N_f - N_q^f + 1, f_q \in \mathbb{N}^* \quad (18)$$

where  $N_q^t$  and  $N_q^f$  mean the time-frequency length of the allocated PRB to uRLLC traffic  $q$  ( $q \leq Q$ ).  $N_f$  is the number of all subcarriers,  $(t_q, f_q)$  is the starting position in time-frequency domain of traffic  $q$ , and all the power allocated to it is denoted as  $p_q$ .  $P_q^{\text{require}}$  and  $d_q$  are the corresponding required BER and latency margin, respectively.  $\alpha$  and  $\beta$  are two parameters used to tune the primary of these two objections.  $\gamma_q$  is the BER of traffic  $q$ . When the power  $p_q$  stays a constant, the maximum  $\gamma_q$  can be obtained from Equation (15) according to the Lagrange Multiplier Method. Equation (11) means the throughput of the eMBB traffic after subtracting that of the uRLLC traffic. Equation (12) infers to total power allocated to the uRLLC traffic. Equation (13) considers the BER demands when multiplexing. Equation (16) means that the PRBs of two different uRLLC traffic get no overlapping parts. Equations (17) and (18) imply that the allocated position of the PRBs are located within the time-frequency limits.

This optimization issue is a NP-hard problem, which is complex to find a certain solution. The heuristic algorithms are often used to solve such questions. Herein, the particle swarm optimization

(PSO) algorithm is employed to deal with it [42]. For each particle, it contains three unsolved variables, i.e.,  $(p_q, t_q, f_q)$ . During the initialization, the initial position and velocity of each particle are randomly generated. If a particle's position satisfies Equations (13), (17), and (18), it is a feasible position that can be used for further process; otherwise an infeasible position will be discarded. After updating the position, Equation (16) is used to check all the position. If a particle's position overlaps with any other's position, then change its position randomly.

Figure 9 presents the simulation results of two multiplexing scheme. Figure 9a shows the PRB positions of different uRLLC traffic (1 for VS, 2 for PIS, 3 for OCS, and 4 for TCS) based on the conventional scheme, i.e., processing the arrived uRLLC traffic in the next mini-slot. In contrast, Figure 9b demonstrates our proposed scheme, where the background color implies the corresponding channel gain (white color refers to a high value).  $\alpha$  and  $\beta$  are set at different value to investigate the primary between the throughput and uRLLC power. The first case focuses on the minimization of the uRLLC power and the corresponding PRB is allocated to time-frequency positions with a high value. The second case puts an emphasis on the minimization of the throughput. As such, the PRB is allocated to time-frequency positions with a low channel gain value. The third case takes both objections into account and yields a relatively compromise result.

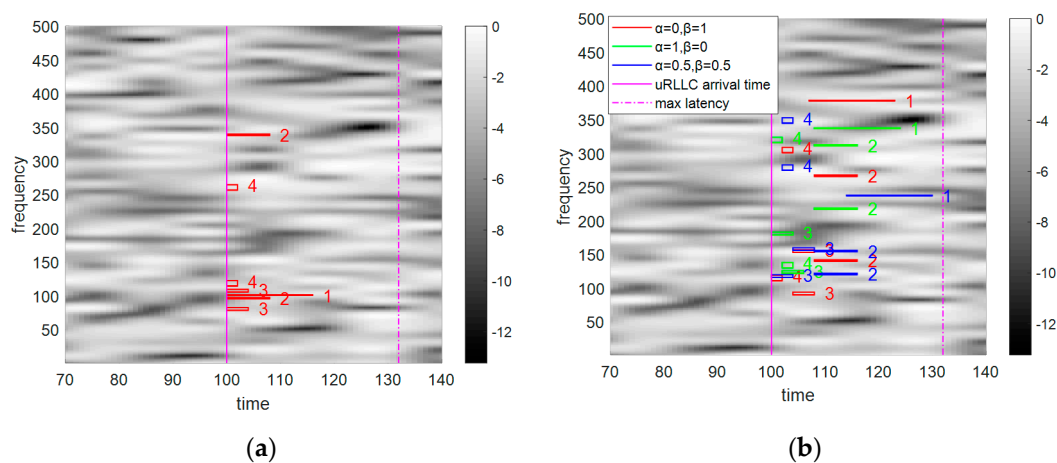


**Figure 9.** A diagram of the PRB positions of uRLLC traffic: (a) the conventional scheme; (b) the proposed scheme.

Based on the above scheme, the coexisting of eMBB and uRLLC traffic can be handled efficiently to maximize the throughput of all eMBB traffic and guarantee the latency as well as BER demands of the uRLLC traffic.

## 6. Passengers Internet Resources Management

The ultra-high-speed not only exerts a heavy impact on the physical wireless channel characterization, but also influences the in-journey passenger Internet access experience. On one hand, the short residence time inside a cell yields a low network throughput. On the other hand, the low-quality wireless channel also decreases the cell throughput to some degree. Generally, the communication system fetches the requested contents from the Internet network through edge cloud and the core network, which consequently generates a large transmission delay, not to mention the transmission latency in the fronthaul, midhaul, and backhaul links. Hence, it is of great importance to investigate resource strategies to improve the QoS at ultra-high-speed.

A promising scheme to boost the communication performance is to add a cache device to the nearby base station (BS) [24,39]. Numerous prevailing pre-fetching methods have been investigated by leveraging the cache equipment. Likewise, we add a cache device to the roadside AAUs to enable the following two cache-based resource management schemes.

### 6.1. Cache-Based Pre-Fetching Scheme

In the conventional pre-fetching scheme, the load balancer will pre-store some popular Internet resources into the cache device preliminarily. As the passengers request for an Internet content, the load balancer will search it in the pre-stored cache first. If found, it will be transmitted to the user instead of being fetched from the Internet via the core network [22]. The conventional cache scheme seems attractive since it can reduce the transmission latency greatly. However, if a passenger requests an un-stored content, the load balancer can do nothing but fetch it from the Internet. Hence, we aim to propose a novel cache-based pre-fetching scheme to deal with such situation.

Generally, the requested contents of small file size can be transferred to users within a short interval. As for those contents of large file size such as the high-definition video (HDV), they usually need a long transmission time, which reduces the communication QoE dramatically. Thanks to the breakpoint transmission technology, a video content of large file size can be chunked into a group of small segments to be independently downloaded and consumed by the Hyperloop on-board passengers. The basic idea of our proposal is to pre-store parts of the requested contents (un-stored in current cache) to the cache of next load balancer as shown in Figure 10. Then the passenger can fetch it directly from the cache as the Hyperloop enters next logical cell. The detailed scheme is formulated as follows:

- (1) As a passenger  $u$  requests for an Internet content, it will arrive at the roadside load balancer first via the wireless link.
- (2) The load balancer searches the requested content in its cache database. If found, then transfer the content to the passengers via the wireless link directly.
- (3) If not found, fetch it from the Internet via the edge cloud. Simultaneously, estimate the transmission completion time  $\Delta t_{complete}$  based on the average allocated data rate mentioned in Equation (15), which can be expressed as

$$\Delta t_{complete} = S_{file} / \bar{R}_u(t), \quad (19)$$

where  $S_{file}$  is the file size of the requested content. Calculate the remaining residence time  $\Delta t_{residence}$  based on Equation (19) inside current logical cell according to Hyperloop position.

- (4) If  $\Delta t_{complete} > \Delta t_{residence}$ , i.e., the requested content will not be transferred to the passenger within the current logical cell completely, broadcast this content request to the nearby edge clouds.
- (5) Assess the burden status of the nearby edge clouds which connects to the load balancer that covers the next logical cell. Select an edge cloud with little communication burden and download the rest part of the requested content from the Internet and store them in the cache of the next load balancer.
- (6) As the Hyperloop enters the next logical cell, the passenger can fetch the remaining transmission-unfinished content from the cache via the wireless link directly.

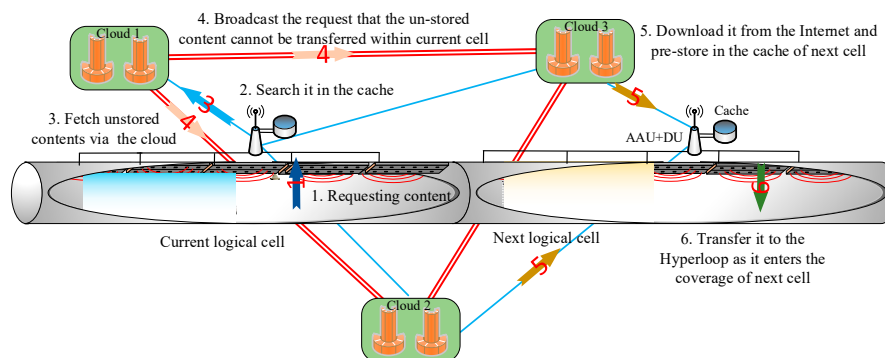
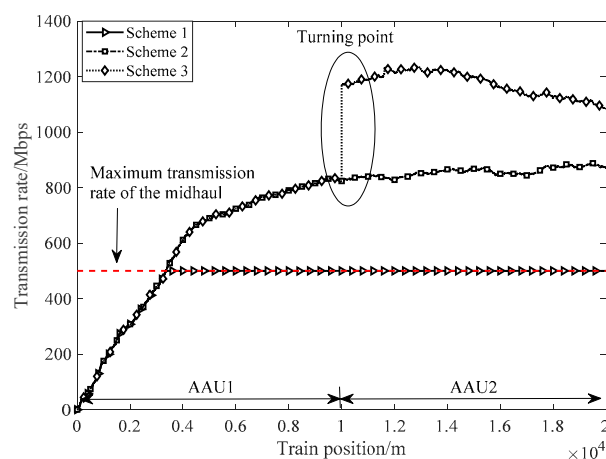


Figure 10. The diagram of the pre-fetching scheme.

In conclusion, we propose a novel pre-fetching scheme by coordinating multiple edge clouds based on the proposed network architecture mentioned in Section 4. The merits of this proposal lie not only in reducing the content transmission delay but also making more margin for the transmission of mission-critical services data.

Figure 11 presents the simulation results of the pre-downloading scheme. The red line denotes the maximum transmission rate of the midhaul, whereas three schemes will be compared, i.e., Scheme 1: without cache, Scheme 2: conventional cache-based strategy (store some popular Internet content in the cache in advance), and Scheme 3: our proposal. The vactrain starts from AAU1 and proceeds across AAU2. The actual throughput of three schemes stays the same in AAU1. Notably, Scheme 3 enables the pre-downloading procedure as the midhaul turns congested. Then, in AAU2, an abrupt throughput ascent of Scheme 3 appears since it pre-downloads some requested contents to the cache. This cache-based scheme presents an inspiring throughput performance especially in terms of the congested wired link.



**Figure 11.** The network throughput at different positions.

## 6.2. Cache-Based Post-Uploading Scheme

As described in Section 2, multi-types of communication services will be transferred via the midhaul link. Usually, the optical-fiber-made midhaul can provide a sufficient bandwidth (in Gb/s) by the wavelength division multiplexing (WDM) technology. However, the processing latency mainly lies in the photoelectric signal conversion, which may endanger the transmission of the mission-critical services. Moreover, the coexistence of multi-types of services implies that several types of traffic attempt to use a common midhaul simultaneously and encounter a data collision [43,44]. As such, high-priority-traffic should be guaranteed first.

The video surveillance data plays a key role in monitoring the Hyperloop real-time status, fault pre-discovery and diagnosis. Data of this type is usually not as latency-sensitive as the other mission-critical data but accounts for a large file size. Therefore, we stagger these data to make more bandwidth for those traffic with higher priorities as shown in Figure 12 [41]. The proposed scheme can be summarized as follows:

- (1) Collect the video surveillance data and transfer it to the nearby load balancer via the wireless link. Then store the data to the cache instead of being forwarded to the cloud center directly.
- (2) Detect the burden status of nearby edge centers and get prepared to forward it to an available edge center with less communication burden. Then transmit the data to an available cloud via the midhaul. This process usually occurs when the Hyperloop has left the current logical cell.

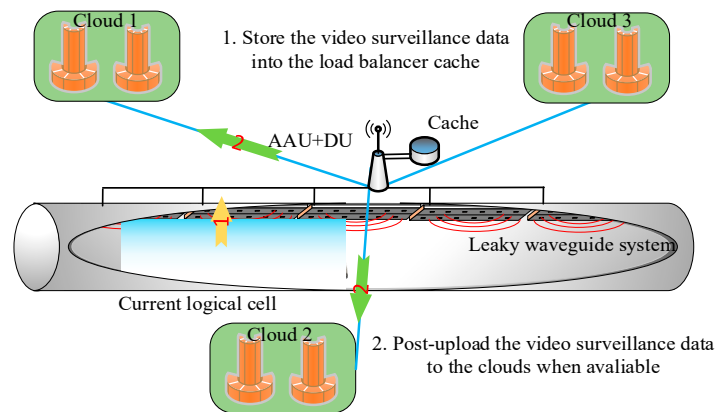


**Figure 12.** The diagram of the post-uploading scheme.

Another issue about these two cache-based schemes is the exact storage size of the cache. It can be roughly estimated that the cache storage size is no larger than

$$S_{cache} = (2F_{frouthal} + F_{wireless})T_{cell}, \quad (20)$$

where the first part means the sum of the pre-fetched file size generated in the previous logical cell and the downloading part in the current cell via the same midhaul. The latter means the maximum uploaded file size via a wireless link when traveling inside the current cell. Based on these two schemes, the network throughput can be greatly improved, and a more reliable link can be established for the transmission of mission-critical services.

## 7. Conclusions

The Hyperloop adopting the magnetic levitation and vacuum tube technologies can achieve an ultra-high-velocity of over 1000 km/h, which brings great challenges to the existing communication systems. In this paper, we propose a train-to-ground wireless communication system solution based on the prevailing 5G system, involving wireless channel, network architecture, resource management. Our contributions together with future works can be summarized as follows:

- (1) The feasibilities of two wireless access methods, i.e., the DAS and LWS, are analyzed. Specifically, the Doppler power spectrums for the DAS at different positions are characterized. Then, we analyze the radio coverage from an aspect of the handover. In future, the accurate radio propagation characterization of the LWS in the near field will be investigated, especially, the Doppler effect of the LWS should be analyzed in detail.
- (2) As for the network structure, C-RAN is utilized to integrate several nearby AAUs into a logical cell, achieving a free-handover effect inside this cell. To deal with the inevitable group handover when traveling across different macro cells, a novel access network structure is investigated to reduce the resource migration cost. However, such proposal can alleviate the cost evidently in the mesh Hyperloop lines, but exerts little impacts on the single sparse Hyperloop line, which will be solved in future.
- (3) In terms of the coexistence of eMBB and uRLLC traffic, we propose a novel PRB multiplexing scheme considering the latency margin of mission-critical services, which aims to maximize the network throughput subject to the stringent requirements of different types of uRLLC traffic. Though we proposed a solution based on the PSO algorithm, an optimization solution with a closed-form expression will be much helpful especially in terms of the low-latency traffic.
- (4) To enhance the QoE of passengers' Internet access, a cache-based mechanism of "staggering the peak" of data transmission (including pre-fetching and post-uploading schemes) is proposed to boost the transmission performance. In the simulation, we only consider the coordination of two

adjacent AAU. However, it can be inferred that the joint of more AAUs will definitely yield a better throughput performance, which will be investigated in the future.

In summary, we make our endeavors to investigate on the train-to-ground communication system for Hyperloop from the aspect of the whole system architecture. We wish our works could enlighten the future research of the Hyperloop.

**Author Contributions:** Conceptualization, J.Z., L.L., T.Z., and B.A.; investigation, J.Z., Z.L., and D.W.; methodology, J.Z., B.H., Z.L., K.W., and B.A.; project administration, L.L.; supervision, L.L.; writing—original draft, J.Z. and L.L.; and writing—review and editing, J.Z. and L.L. All authors have read and agreed to the published version of the manuscript.

**Funding:** This research was supported by the Fundamental Research Funds for the Central Universities under grant 2018JBZ102, and the Beijing Nova Programme Interdisciplinary Cooperation Project (Z191100001119016).

**Acknowledgments:** The authors thank the anonymous reviewers for their constructive comments which are much helpful for enhancing the quality and presentation of this paper.

**Conflicts of Interest:** The authors declare no conflict of interest.

## References

- Guan, K.; Ai, B.; Peng, B.L.; He, D.P.; Li, G.K.; Yang, J.Y.; Zhong, Z.D.; Kürner, T. Towards realistic high-speed train channels at 5G millimeter-wave band—Part I: Paradigm, significance analysis, and scenario reconstruction. *IEEE Trans. Veh. Technol.* **2018**, *67*, 9112–9128. [[CrossRef](#)]
- Zhou, T.; Tao, C.; Salou, S.; Liu, L. Geometry-Based Multi-Link Channel Modeling for High-Speed Train Communication Networks. *IEEE Trans. Intell. Transp. Syst.* **2020**, *21*, 1229–1238. [[CrossRef](#)]
- Qiu, C.C.; Liu, L.; Liu, Y.; Li, Z.; Zhang, J.C.; Zhou, T. Key Technologies of Broadband Wireless Communication for Vacuum Tube High-Speed Flying Train. In Proceedings of the 2019 IEEE 89th Vehicular Technology Conference, Kuala Lumpur, Malaysia, 28 April–1 May 2019.
- Ahmed, S.A.; Jawwad, S.; Mohamed, Z.Y. Hyperloop Transportation System: Analysis, Design, Control, and Implementation. *IEEE Trans. Ind. Electron.* **2018**, *65*, 7427–7436. [[CrossRef](#)]
- Hyperloop Alpha. Available online: [https://spacex.com/sites/spacex/files/Hyperloop\\_alpha.pdf](https://spacex.com/sites/spacex/files/Hyperloop_alpha.pdf) (accessed on 26 April 2020).
- We Ran the Numbers on a European Hyperloop—And They Look Fantastic. Available online: <https://Hyperloop-one.com/blog/we-ran-the-numbers-on-euro-Hyperloop> (accessed on 26 April 2020).
- We Made History Two Minutes after Midnight On May 12. Available online: <https://Hyperloop-one.com/blog/we-made-history-two-minutes-after-midnight-may-12> (accessed on 26 April 2020).
- Hyperloop TT Begins Construction of its First Test Track. Available online: <https://www.engadget.com/2018/04/12/Hyperloop-tt-begins-construction-of-its-first-test-track/> (accessed on 26 April 2020).
- China Sets Key Tasks for Building National Strength in Transportation. Available online: <http://global.chinadaily.com.cn/a/201909/25/WS5d8acb25a310cf3e3556d5b6.html> (accessed on 26 April 2020).
- TÜV SÜD Publishes Safety Guidelines for Hyperloop Applications. Available online: <https://www.tuvsud.com/en/press-and-media/2020/july/tuev-sued-publishes-safety-guidelines-for-hyperloop-applications> (accessed on 14 August 2020).
- He, R.S.; Ai, B.; Wang, G.P.; Guan, K.; Zhong, Z.D.; Molisch, A.F.; Rodriguez, C.B.; Oestges, C.P. High-Speed Railway Communications: From GSM-R to LTE-R. *IEEE Veh. Technol. Mag.* **2016**, *11*, 49–58. [[CrossRef](#)]
- Yang, J.K.; Boyd, J.; Laney, D.; Schlenzig, J. Next Generation Half-Duplex Common Data Link. In Proceedings of the IEEE Military Communications Conference, Orlando, FL, USA, 29–31 October 2007.
- Qiu, C.C.; Liu, L.; Han, B.T.; Zhang, J.C.; Li, Z.; Zhou, T. Broadband Wireless Communication Systems for Vacuum Tube High-Speed Flying Train. *Appl. Sci.* **2020**, *10*, 1379. [[CrossRef](#)]
- Zhang, J.C.; Liu, L.; Li, Z.; Zhou, T.; Qiu, C.C.; Han, B.T.; Wang, D.; Piao, Z.Y. Two Novel Structures of Broadband Wireless Communication for High-speed Flying Train in Vacuum Tube. In Proceedings of the 2019 28th Wireless and Optical Communications Conference (WOCC), Beijing, China, 9–10 May 2019.
- Han, B.T.; Zhang, J.C.; Liu, L.; Tao, C. Position-Based Wireless Channel Characterization for the High-Speed Vactrains in Vacuum Tube Scenarios Using Propagation-Graph Modeling Theory. *Radio Sci.* **2020**, *55*, e2020RS007067. [[CrossRef](#)]

16. Han, B.T.; Liu, L.; Zhang, J.C.; Tao, C.; Qiu, C.C.; Zhou, T.; Li, Z.; Piao, Z.Y. Research on Resource Migration Based on Novel RRH-BBU Mapping in Cloud Radio Access Network for HSR Scenarios. *IEEE Access* **2019**, *7*, 108542–108550. [[CrossRef](#)]
17. Wang, K.; Liu, L.; Han, B.T.; Zhang, J.C.; Tao, C.; Li, Z. High-Speed Railway Communication Based on Dynamic Mapping of BBU-RRH Using Cloud Radio Access Network. In Proceedings of the 2019 IEEE 5th International Conference on Computer and Communications (ICCC), Chengdu, China, 6–9 December 2019.
18. Lien, S.Y.; Shieh, S.L.; Huang, Y.; Su, B.; Hsu, Y.L.; Wei, H.Y. 5G New Radio: Waveform, Frame Structure, Multiple Access, and Initial Access. *IEEE Commun. Mag.* **2017**, *55*, 64–71. [[CrossRef](#)]
19. Alsenwi, M.; Tran, N.H.; Bennis, M.; Bairagi, A.K.; Hong, C.S. eMBB-URLLC Resource Slicing: A Risk-Sensitive Approach. *IEEE Commun. Lett.* **2019**, *23*, 740–743. [[CrossRef](#)]
20. Darabi, M.; Lampe, L. Multi Objective Resource Allocation for Joint eMBB and URLLC Traffic with Different QoS Requirements. In Proceedings of the 2019 IEEE Globecom Workshops (GC Wkshps), Waikoloa, HI, USA, 9–13 December 2019.
21. Anand, A.; Veciana, G.D.; Shakkottai, S. Joint Scheduling of URLLC and eMBB Traffic in 5G Wireless Networks. In Proceedings of the IEEE Conference on Computer Communications, Honolulu, HI, USA, 15–19 April 2018.
22. Cao, Y.; Wang, N.; Wu, C.; Zhang, X.; Suthaputchakun, C. Enhancing Video QoE Over High-Speed Train Using Segment-Based Prefetching and Caching. *IEEE MultiMed.* **2019**, *26*, 55–66. [[CrossRef](#)]
23. Zhang, Z.Z.; Chen, Z.Y.; Xia, B. Cache-Enabled Uplink Transmission in Wireless Small Cell Networks. In Proceedings of the 2018 IEEE International Conference on Communications (ICC), Kansas City, MO, USA, 20–24 May 2018.
24. Zhang, J.C.; Liu, L.; Wang, K.; Piao, Z.Y.; Zhou, T. A Cache-Based Pre-Downloading Scheme for HSR Communication Using C-RAN. In Proceedings of the The 8th IET International Conference on Wireless, Mobile & Multimedia Networks, Beijing, China, 15–17 November 2019.
25. Liu, L.; Tao, C.; Qiu, J.H.; Chen, H.J.; Yu, L.; Dong, W.H.; Yuan, Y. Position-Based Modeling for Wireless Channel on High-Speed Railway under a Viaduct at 2.35 GHz. *IEEE J. Sel. Areas Commun.* **2012**, *30*, 834–845. [[CrossRef](#)]
26. Shafi, M.; Molisch, A.F.; Smith, P.J.; Haustein, T.; Zhu, P.Y.; Silva, D.P.; Tufvesson, F.; Benjebbour, A.; Wunder, G. 5G: A Tutorial Overview of Standards, Trials, Challenges, Deployment, and Practice. *IEEE J. Sel. Areas Commun.* **2017**, *35*, 1201–1221. [[CrossRef](#)]
27. Masson, É.; Berbineau, M. *Broadband Wireless Communications for Railway Applications*; Springer International: Berlin/Heidelberg, Germany, 2017.
28. Zhou, M. Analysis on the technical characteristics of wireless communication between vehicles and grounds of Shanghai Maglev line. *Urban Mass Transit* **2010**, *13*, 26–29. (In Chinese)
29. Zhong, Z.D.; He, R.S.; Guan, K.; Ai, B.; Zhu, G.; Lei, L.; Wang, F.G.; Ding, J.W.; Xiong, L.; Wu, H. *Dedicated Mobile Communications for High-Speed Railway*; Springer: Berlin/Heidelberg, Germany, 2017.
30. Tian, L.; Degli-Esposti, V.; Vitucci, E.M.; Yin, X.F. Semi-Deterministic Radio Channel Modeling Based on Graph Theory and Ray-Tracing. *IEEE Trans. Antennas Propag.* **2016**, *64*, 2475–2486. [[CrossRef](#)]
31. Heddebaut, M. Leaky Waveguide for Train-to-Wayside Communication-Based Train Control. *IEEE Trans. Veh. Technol.* **2009**, *58*, 1068–1076. [[CrossRef](#)]
32. Wang, H.W.; Yu, F.R.; Jiang, H.L. Modeling of Radio Channels with Leaky Coaxial Cable for LTE-M Based CBTC Systems. *IEEE Commun. Lett.* **2016**, *20*, 1038–1041. [[CrossRef](#)]
33. Wang, J.H.; Mei, K.K. Theory and Analysis of Leaky Coaxial Cables with Periodic Slots. *IEEE Trans. Antennas Propag.* **2001**, *49*, 1723–1732. [[CrossRef](#)]
34. Hrovat, A.; Kandus, G.; Javornik, T. A Survey of Radio Propagation Modeling for Tunnels. *IEEE Commun. Surv. Tutor.* **2014**, *16*, 658–669. [[CrossRef](#)]
35. Cho, H.; Shin, S.; Lim, G.; Lee, C.; Chung, J.-M. LTE-R Handover Point Control Scheme for High-Speed Railways. *IEEE Wirel. Commun.* **2017**, *24*, 112–119. [[CrossRef](#)]
36. Zhao, J.H.; Liu, Y.Y.; Gong, Y.; Wang, C.Y.; Fan, L.S. A Dual-Link Soft Handover Scheme for C/U Plane Split Network in High-Speed Railway. *IEEE Access* **2018**, *6*, 12473–12482. [[CrossRef](#)]
37. Song, H.; Fang, X.M.; Yan, L. Handover Scheme for 5G C/U Plane Split Heterogeneous Network in High-Speed Railway. *IEEE Trans. Veh. Technol.* **2014**, *63*, 4633–4646. [[CrossRef](#)]

38. Checko, A.; Christiansen, H.L.; Yan, Y.; Scolari, L.; Kardaras, G.; Berger, M.S.; Dittmann, L. Cloud RAN for Mobile Networks—A Technology Overview. *IEEE Commun. Surv. Tutor.* **2015**, *17*, 405–426. [[CrossRef](#)]
39. Parvez, I.; Rahmati, A.; Guvenc, I.; Sarwat, A.I.; Dai, H.Y. A Survey on Low Latency Towards 5G: RAN, Core Network and Caching Solutions. *IEEE Commun. Surv. Tutor.* **2018**, *20*, 3098–3130. [[CrossRef](#)]
40. Kitindi, E.J.; Fu, S.; Jia, Y.J.; Kabir, A.; Wang, Y. Wireless Network Virtualization with SDN and C-RAN for 5G Networks: Requirements, Opportunities, and Challenges. *IEEE Access* **2017**, *5*, 19099–19115. [[CrossRef](#)]
41. Iftikhar, Z.; Jangsher, S.; Qureshi, H.K.; Aloqaily, M. Resource Efficient Allocation and RRH Placement for Backhaul of Moving Small Cells. *IEEE Access* **2019**, *7*, 47379–47389. [[CrossRef](#)]
42. Gong, Y.J.; Zhang, J.; Chung, H.S.; Chen, W.N.; Zhan, Z.H.; Li, J.; Shi, Y.H. An Efficient Resource Allocation Scheme Using Particle Swarm Optimization. *IEEE Trans. Evol. Comput.* **2012**, *16*, 801–816. [[CrossRef](#)]
43. Peng, M.G.; Wang, C.G.; Lau, V.; Vincent Poor, H. Fronthaul-constrained cloud radio access networks: Insights and challenges. *IEEE Wirel. Commun.* **2015**, *22*, 152–160. [[CrossRef](#)]
44. Liang, H.; Zhang, W.H. Efficient On-Demand Data Service Delivery to High-Speed Trains in Cellular/Infostation Integrated Networks. *IEEE J. Sel. Areas Commun.* **2012**, *30*, 780–791. [[CrossRef](#)]



© 2020 by the authors. Licensee MDPI, Basel, Switzerland. This article is an open access article distributed under the terms and conditions of the Creative Commons Attribution (CC BY) license (<http://creativecommons.org/licenses/by/4.0/>).